Scaling laws of the additive random-matrix model

Georg Lenz, Karol Życzkowski,* and Dirk Saher
Fachbereich Physik, Universität Gesamthochschule Essen, 4300 Essen, Federal Republic of Germany
(Received 9 April 1991)

The scaling behavior of the additive random-matrix model $H=(H^0+\lambda V)/(1+\lambda^2)^{1/2}$ has been investigated. This model, capable of producing transitions between different degrees of level repulsion for the eigenvalues, has been analyzed for the case of the transition from the Poisson distribution $\exp(-S)$ of the distances between adjacent eigenvalues to the Wigner distribution $(\pi S/2)\exp(-S^2\pi/4)$. We propose expressions for the level-spacing distribution and the distribution of the eigenvector components and demonstrate their reliability by means of numerical computations. For the eigenvalues, the transition proceeds at a rate that scales as the square root of the matrix dimension. For the eigenvalues, the rate is independent of this dimension.

PACS number(s): 05.45.+b, 02.50.+s, 24.60.Ky

I. INTRODUCTION

When physicists started to investigate the properties of nuclei systemically, they realized very early that it is hardly possibly to explain the vast complexity of the level scheme or the fluctuations of the cross sections of neutron scattering by means of first-principles calculations. So they studied properties of the eigenvalue spectrum and the fluctuations of the transition strengths and cross sections. Much attention was paid to the distribution of nearest-neighbor spacing [1,2] between eigenvalues $S=(e_{i+1}-e_i)\langle\rho\rangle$, (the multiplication with the mean level density $\langle\rho\rangle$ is used to normalize $\langle S\rangle$ to unity). One also studies the distribution of transition strengths, i.e., the elements of the transition matrix $y=|\langle\Phi|\hat{T}|\varphi_i\rangle|^2$ between a fixed state $|\Phi\rangle$ and eigenvectors $\{|\varphi_i\rangle, i=1,\ldots,N\}$, which span the Hilbert space. This structure of y suggests that one may combine $\hat{T}$ and $|\Phi\rangle$ to a new unknown, but fixed, vector $|\tilde{\Phi}\rangle$. One confronts, therefore, a problem of describing the statistical properties of the eigenvectors $\{|\varphi_i\rangle, i=1,\ldots,N\}$ of a Hamilton operator H in a certain basis [3]. For both distributions expressions were surmised [1,2].

$$P(S)=(\pi S/2)\exp(-S^2\pi/4), \tag{1a}$$

$$P(y)=\frac{1}{\sqrt{2\pi\langle y\rangle}}e^{-y/2\langle y\rangle}. \tag{1b}$$

The first one has come to be called the Wigner surmise, the second one the Porter-Thomas distribution. The quantity $\langle y\rangle$ is the mean value of the transition strengths. It defines the scale of statistics and can therefore be set to unity. It is now understood that these original propositions apply not only to nuclear Hamiltonians but to a whole universality class of dynamical systems. That class is referred to as *orthogonal* and is characterized by Hamiltonians which (i) generate globally chaotic motion in the classical limit and (ii) are time-reversal invariant. It is represented by an ensemble of real symmetric random matrices [Gaussian orthogonal ensemble (GOE)] [4]. Two other quantum-mechanical universality classes are associated with the global classical chaos: the *unitary* ensemble with the systems with no time-reversal symmetry [4,5] and the *symplectic* ensemble with systems with Kramers degeneracy and no additional parity [4,6]. For both classes, generalizations of Eq. (1) exist [4].

The fact that the statistical description of classically chaotic systems is possible in terms of random matrices is astonishing and needs two clarifying remarks. First, Hamiltonians of dynamical systems mostly do not appear to be random. In fact the equivalence of spectral fluctuations for random and "nonrandom" Hamiltonians has been understood only recently [7]. Second, the equivalence of a spectral average of some quantity (e.g., the eigenvalue density in a given spectrum of a matrix M) for one matrix M member of an ensemble, to an ensemble average over all matrices of the ensemble, is a nontrivial property of the ensemble that is often hard to prove [8].

A fourth universality class we need to mention here comprises classical integrable systems with two or more degrees of freedom. In that class, levels do not repel but rather tend to cluster together so as to give rise to an exponential distribution of nearest-neighbor spacings [9] $P(S)=e^{-S}$. In that respect, the levels behave like the uncorrelated events of a random Poisson process.

We shall be concerned here with the Hamiltonians "in between" two universality classes for integrable and for fully chaotic systems (with time-reversal symmetry). The investigation of the nature of the eigenvalue spectrum of these Hamiltonians is of great interest, because it is a keystone to understanding quantum chaos. Berry and Robnik [10] have proposed a distribution of nearest-neighbor spacings for these systems. Motivated by semiclassical ideas, they presented a family of distributions which interpolate between the Poisson and the Wigner distributions. Even earlier Brody [2] proposed to use the Weibull distribution, well known in statistical analysis, to describe the transition from Poisson to Wigner-like spectra. Astonishingly, this proposition, which involved only the assumption that the level repel $\sim S^{\omega}$, $\omega\in[0,1]$, seems to have had the greatest success in fitting experimental and numerical data. Parallel to the change in the level repul-

sion, a transition in the distribution of transition strengths takes place [11]. This phenomenon, in a slightly different context, has already been utilized to give an upper bound on the time-reversal noninvariant part of the nucleon-nucleon interaction [12].

At present, the discussion about the right random matrix ensemble describing the transition from a Poisson to a Wigner spectrum is not over. Recently, Feingold *et al.* [13,14] used semiclassical arguments to define an ensemble of band matrices. In the limiting case of this ensemble, which corresponds to the analog of classically ergodic systems, the GOE fluctuation properties of the spectrum were observed. A similar band random-matrix model was investigated by Casati *et al.* [15]. Interesting scaling laws during the localization-delocalization transition were found for eigenvalues [16] and eigenvectors [17]. Other papers use models of full random matrices to describe the Hamiltonians in between the universality classes [18,19]. This line will be followed in our work.

The aim of this paper is to describe the simplest random-matrix model capable of describing Hamiltonians of the transition between a Poisson and a Wigner spectrum. Our investigation provides information about the eigenvalue and eigenvector statistics of this model, so far not presented. One reason for reporting these facts is to verify and complete some results recently reported by Cheon [20].

This paper will be organized as follows. In Sec. II, we will describe our model. In Sec. III we discuss the statistical properties of eigenvalues and present some numerical results; in Sec. IV, we do the same for eigenvectors. We conclude, in Sec. V, by summarizing our results and discuss their possible applications and the connection with band random-matrix models.

II. MODEL

For most dynamical systems which have a mixed phase space (a Poincaré section shows the Kolmogorov-Arnold-Moser tori and chaotic layers), it is possible to change the fraction of the chaotic volume in the phase space continuously from zero to one by increasing a single parameter in the Hamiltonian. One can write a Hamiltonian H,

$$H=H^0+\lambda V, \tag{2}$$

where H^0 describes a regular system and V is a perturbation causing a transition to globally chaotic motion. In a different context, Hamiltonians of the form of Eq. (2) are studied in nuclear physics. One often faces the problem of estimating the "size" of a symmetry-breaking (e.g., isospin) or time-reversal-breaking part in a Hamiltonian necessary to produce a sizable effect on the spectrum. In this situation, V breaks the symmetry and λ plays the role of the strength of symmetry-breaking part when H^0 and V have the same norm [12,18,19]. In this situation one generally has no knowledge of the microscopic structure of H^0 and V, but it is known that the statistical behavior of the nearest-neighbor spacings of the spectra for Hamiltonians belonging to different symmetry classes are different [1]. The simplest way to study the transition in the spectra is to choose H^0 and V from different classes. To go even a step further, one can select both from different random-matrix ensembles, constructed with the only condition of preserving a certain symmetry [1,2].

Problems motivated by "quantum chaos" lead to a different situation since, in most cases, one has detailed knowledge of H^0 and V. The justification for choosing H^0 and V from different random-matrix ensembles and to study the transition from the GOE spectrum to the Gaussian unitary ensemble spectrum for a globally chaotic system, or from the Poisson to the GOE spectrum by studying Eq. (2), was given only recently [21].

For our specific purpose, we choose V from the GOE ensemble of real symmetric $N\times N$ matrices and H^0 as a diagonal matrix with a Gaussian distribution (with mean equal to zero) of all elements. For $\lambda=0$ we get the Poisson distribution of the nearest-neighbor spacings and for $\lambda\to\infty$ the Wigner surmise Eq. (1a). To keep the eigenvalues of H in a bounded range of the energy axis, we slightly modify [21] Eq. (2):

$$H=(H^0+\lambda V)/\sqrt{1+\lambda^2}\ . \tag{3}$$

To complete our definition, we choose the following variances for the matrix elements:

$$\begin{aligned}&\langle (H^0_{ij})^2\rangle=\delta_{ij}\ ,\\ &\langle V^2_{ii}\rangle=2\langle V^2_{ij}\rangle=1/2N,\quad i\neq j,\end{aligned} \tag{4}$$

where the brackets denote the ensemble average. We are interested in large matrices, $N\gg 1$.

III. EIGENVALUES

We are interested in the eigenvalue distribution of the ensemble defined above.

The probability density $P(H,\lambda)$ is given by

$$P(H\lambda)=\langle \delta(H-(H^0+\lambda V)/\sqrt{1+\lambda^2})\rangle. \tag{5}$$

Let us start with a few remarks about the density of the eigenvalues. For $\lambda=0$, we get a zero-centered Gaussian with the variance equal to 1 while, for $\lambda\to\infty$, we approach a semicircle [22] with radius equal to 1. Figure 1 shows the integrated density for three different values of λ. Each curve was generated by superimposing spectra of 100 200×200 matrices. For later comparison we draw attention to the values of λ needed to complete the transition. The density performs its transition on a "time scale" λ_d one order of $\sqrt{N}$ slower than the spacing distribution [23], so during the whole transition of the spacing distribution from Poisson to Wigner we may assume that the density remains Gaussian.

A first step towards the description of the spacing distribution for the ensemble (5) is to consider the case [24] of $N=2$. Let us take for H^0 an ensemble of real symmetric 2×2 matrices of the form

$$\begin{aligned}P(H^0)=&\exp\{-[(\mathrm{Tr}H^0)^2-4\,\mathrm{Det}H^0]^{1/2}\}\exp[-\mathrm{Tr}(H^0)^2]\\ &\times[(\mathrm{Tr}H^0)^2-4\,\mathrm{Det}H^0]^{-1/2}\ ,\end{aligned} \tag{6}$$

and, for V, a 2×2 GOE ensemble. The first ensemble is easily seen to imply an exponential distribution of the spacing between the two eigenvalues. The averages in Eq.

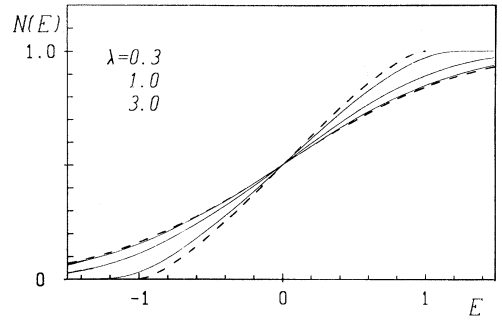

FIG. 1. For fixed λ we sampled the eigenvalues of 100 200×200 matrices and plotted the integrated density $N(E)$. The dashed lines indicate the corresponding expression, $1+\mathrm{erf}(E/\sqrt{2})/2$, for $\lambda=0$ and the semicircle with radius unity for $\lambda=\infty$.

(5) can now be done explicitly. The resulting matrix density depends on H^0 through three real variables H^0_{11}, H^0_{12}, and H^0_{22}. By a suitable double integral we arrive at the spacing distribution, which can be expressed in terms of the modified Bessel function $I_0(x)$ and the Tricomi function [25] $U(a,b,x)$ as

$$P(S,\lambda)=\left[\frac{Su(\lambda)^2}{\lambda}\right]\exp\left[\frac{-u(\lambda)^2S^2}{4\lambda^2}\right]$$

$$\times\int_0^\infty e^{(-\xi^2-2\xi\lambda)}I_0\left[\frac{S\xi u(\lambda)}{\lambda}\right]d\xi, \qquad (7)$$

where $u(\lambda)=\sqrt{\pi}U(-1/2,0,\lambda^2)$. For $\lambda=0$, the above distribution reduces to Poissonian e^{-S} while the Wigner surmise Eq. (1a) is approached in the limit $\lambda\to\infty$. For all intermediate values of λ, we encounter linear repulsion of eigenvalues, i.e., $P(S,\lambda)\sim S/\lambda$, for $S<\lambda\ll1$. Figure 2 presents distributions (7) for some different values of the control parameter λ. Note that the overshooting of the analyzed distribution over the Poisson curve of small values of λ is significantly different from the behavior of the Brody or Berry-Robnik distributions.

Equation (7) is exact only for 2×2 matrices, but we could also show its reliability for large matrices of the form (3) and (4) with various values of N and λ. In order

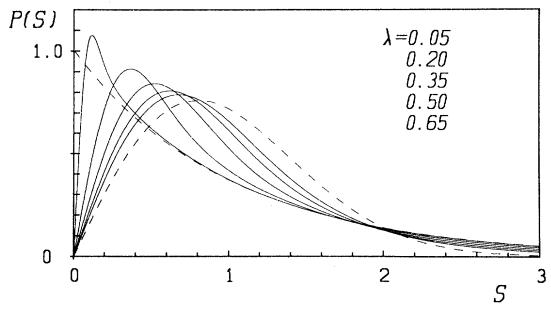

FIG. 2. Spacing distribution for the 2×2 ensemble, interpolating between the Poisson distribution and the Wigner surmise.

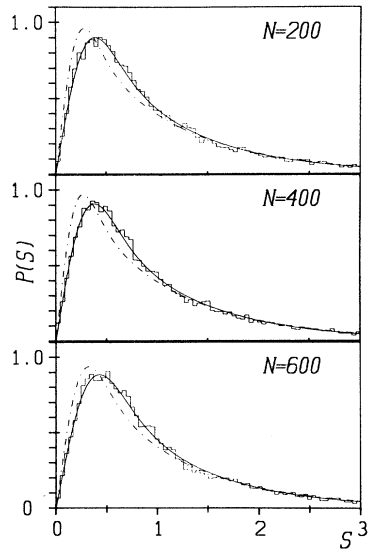

FIG. 3. Histograms obtained from the eigenvalues at the center of the spectrum, for three different matrix dimensions, together with the best-fitting curve from family (7). Parameters from top to bottom: $N=200$, $\lambda=0.075$, $\lambda_{\mathrm{fit}}=0.219$; $N=400$, $\lambda=0.05$, $\lambda_{\mathrm{fit}}=0.210$; $N=600$, $\lambda=0.05$, $\lambda_{\mathrm{fit}}=0.251$. The dashed curve shows the spacing distribution in the wings of the spectra; $\tilde{\lambda}_{\mathrm{fit}}=0.142$, $\tilde{\lambda}_{\mathrm{fit}}=0.133$, $\tilde{\lambda}_{\mathrm{fit}}=0.169$.

to find an optimal method of analysis of the numerically obtained spectra, we tried the techniques of spectral and ensemble unfolding [26,27]. The method of spectral unfolding seems to be the most appropriate one for the case at hand since it suppresses "spurious fluctuations." Even after this unfolding procedure, the spacing statistics depends on the part of the energy axis from which the eigenvalues are taken. This property was expected since the fluctuations in different parts of the spectrum undergo the transition from level clustering to level repulsion at different rates, proportional to the local densities [23]. That inhomogeneity of the matrix ensemble in consideration is least pronounced near $E=0$, where the level density depends most weakly on E. As a consequence, we used only a part of the spectrum around $E=0$, always

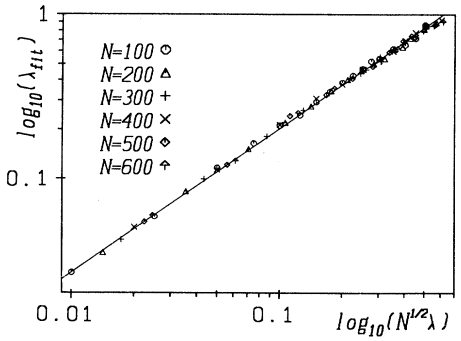

FIG. 4. Scaling behavior of the transition parameter λ_{fit}, obtained through fitting the 2×2 spacing distribution on histograms, as a function of the bare λ in the random-matrix model.

collecting ~15 000 spacings. We thoroughly checked that the remaining inhomogeneity exerts no significant influence on our results.

With all these precautions taken, we have found the numerically determined spacing distributions to be faithful to our proposition (7) to an amazingly high degree of accuracy throughout the transition. In Fig. 3 we present histograms drawn from ensembles of different matrix dimensions together with the best-fitting curve from the family of distributions (7). To have an objective criterion for the quality of the fits, we used a 5% χ-square test. The quality of the fit with Eq. (7) was, for all N and all λ, as good a fit as a GOE spectrum, of the same number of eigenvalues, with the Wigner surmise Eq. (1a). This means that we are able to discriminate the different spacing distributions in different parts of the spectrum. It should be noted here that the best-fit value $\lambda_{\rm fit}$ of the parameter in the distribution (7) does not necessarily coincide with the control parameter λ defining the transition in the ensemble (3). The fitting parameter $\lambda_{\rm fit}$ depends, in fact, on the part of the spectrum from which the histogram was made. The solid lines in Fig. 3 represent the best fit obtained for data from the center of the spectrum while the dashed lines denote fits done for the wings.

In Ref. [23] it was argued that the transition should proceed at a rate $\sim\sqrt{N}$. To study the transition rate, we have plotted the logarithm of the fitting parameter $\lambda_{\rm fit}$ against the logarithm of $\lambda\sqrt{N}$, where λ is the bare value of the control parameter in definition (3). Convincing results are presented in Fig. 4. A direct comparison with the results of Cheon [20] becomes easier by using his method of the analysis of the distribution's momentum. In Fig. 5 we present our results in the momentum-momentum plot. Contrary to his results, all points for all values N and λ lay on a single line. Moreover, this line might be well approximated by a curve calculated from our proposition (7). Such an agreement seems to provide a convincing argument for the existence of scaling in our model. Slight systematic deviations of the numerical results from our curve for small values of λ are a consequence of a little drawback of the method of spectral unfolding. The Poisson spectrum is not invariant under this procedure. The resulting distribution differs from the Poissonian: it has a finite range and an algebraic falloff.

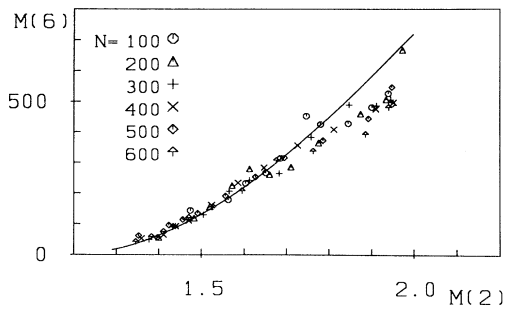

FIG. 5. Plot of the sixth moment $\langle S^6\rangle(\lambda)$ as a function of the second $\langle S^2\rangle(\lambda)$ during the transition from the Poisson spectrum (upper right corner) to the GOE spectrum (lower left corner). Details in text.

The moments of this distribution can be calculated analytically and they agree exactly with the numerical data in the case of $\lambda \ll 1$. Details are given in the Appendix.

IV. EIGENVECTORS

We have also studied the eigenvector statistics of the matrices belonging to the ensemble Eq. (5). Numerical diagonalization of a matrix provides N eigenvectors $\{\psi_k, k=1,\ldots,N\}$, each described by N components $\{c_k^l, l=1,\ldots,N\}$. We are interested in the distribution of squared components $y=|c_k^l|^2$. It is well known [2,4] that, for the pure orthogonal ensemble ($\lambda\to\infty$) for the case of large N the probability $P(y)$ is given by the so-called Porter-Thomas distribution (1b). Figure 6 presents the statistics $P(\log_{10}(y))$ (on the logarithmic scale) for $N=200$ and different values of λ. Each histogram was built of data from 20 matrices to assure a sufficient statistics. Values of y are scaled in such a way as to keep

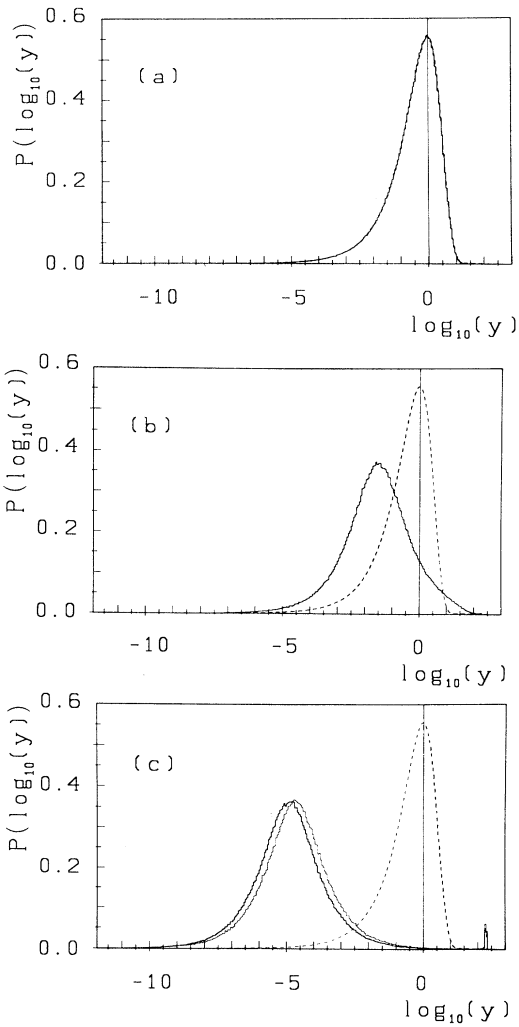

FIG. 6. Eigenvector statistics for $N=200$ and $\lambda=12.0$ (a), 0.50 (b), and 0.01 (c). Dashed lines denote GOE prediction. The narrow line in (c) represents the histogram of eigenvectors which correspond to eigenvalues in the center of the spectrum.

$\langle y \rangle = 1$, so the Porter-Thomas distribution has the maximum at $\log_{10}(y)=0$. For $\lambda=12.0$ [Fig. 6(a)], the numerical results coincide so well with the Porter-Thomas distribution that one can hardly distinguish between the histogram and the dashed line, representing Eq. (1b). With smaller values of λ, the distribution $P(\log_{10}(y))$ becomes wider and almost symmetric. The maximum of the distribution y_m is shifted toward smaller values of y. Such a distribution, obtained for $\lambda=0.5$, is presented in Fig. 6(b). For even smaller values of λ [0.01 at Fig. 6(c)], the distribution is shifted further and y_m decreases, while at $\log_{10}(y)=\log_{10}(N)$ a peak appears, which corresponds to the diagonal elements. In the limit $\lambda \to 0$, the matrix c_k^1 is equal to the identity matrix, the main peak of the distribution escapes to the left as $\log_{10}(y) \to -\infty$, and only the peak at $\log_{10}(N)$ remains.

In order to estimate the inhomogeneity along the energy axis, we have selected only those eigenvectors which correspond to eigenvalues lying in the center of the spectrum, and prepared a separate statistics for them. The narrow histogram in Fig. 6(c) shows the eigenvector statistics obtained from 50% of all eigenstates for the same value of $\lambda=0.01$. Eigenvectors from the center of the spectrum are slightly more delocalized than the average, but the difference in the distribution is not very large. The discussed eigenvector statistics possess an interesting feature. Its dependence on the size N of the matrices is almost negligible, apart from the peak at $\log_{10}(N)$ which occurs for sufficiently small λ. The shape of the main peak of the distribution seems not to change for wide ranges of N and λ, so the distribution may be characterized by the position of the maximum y_m. Figure 7 presents the dependence $\log_{10}(y_m)$ on $\log_{10}(\lambda)$ for different size of matrices. The number of matrices diagonalized was changed in order to keep the total number of components $>10^5$. Even though N varies from 2 to 600, all points lie close to a straight line with fitted slope equal to 1.96. Hence, the main peak of the distribution $P(\log_{10}(y))$ moves right with $y_m \sim \lambda^2$ independently on the matrix size N. The value $\log_{10}(\lambda_c)=0.5$ at which the fitted line intersects the axis $\log_{10}(y_m)=0$ gives a good approximation for the critical value of the parameter λ necessary to obtain the vector statistics in agreement with the prediction of the orthogonal ensemble.

The fact that the eigenvector statistics does not depend significantly on N enables us to look for an approximation for the distribution $P(y)$ by analyzing 2×2 matrices. Consider a symmetric matrix

$$A=\begin{bmatrix} a & x \\ x & a+b \end{bmatrix} \tag{8}$$

and the orthogonal matrix O, such that $\hat{A}=O^{\dagger}AO$ is diagonal. This constraint determines y, the squared nondiagonal element of O,

$$y=|O_{12}|^2=\frac{1}{2}\left[1-\frac{1}{\sqrt{1+4x^2/b^2}}\right]. \tag{9}$$

Since we are interested in the regime of small λ so $x^2 \ll b^2$, the quantity y can be approximated by

$$y \approx \frac{x^2}{b^2+2x^2} \approx \frac{x^2}{b^2}. \tag{10}$$

According to the definition of the model, the variable $\xi=x^2$ is distributed with the Porter-Thomas distribution with the mean value $\langle \xi \rangle = \langle H_{ij}^2 \rangle$, $i \neq j$, and the random variable $\mu=b^2$ has the same distribution with mean value $\langle \mu \rangle = 2\langle H_{ii}^2 \rangle$. The distribution $P(y)$ may thus be approximated by

$$P(y)=\int_0^{\infty}\int_0^{\infty}\delta(y-\xi/\mu)\frac{e^{-\xi/2\langle\xi\rangle}e^{-\mu/2\langle\mu\rangle}}{2\pi\sqrt{\langle\xi\rangle\langle\mu\rangle\xi\mu}}d\xi\,d\mu. \tag{11}$$

Performing integrations and substituting variances $\langle H_{ii}^2 \rangle$ and $\langle H_{ij}^2 \rangle$ from Eq. (4), we obtain

$$P(y)=\frac{2\lambda\sqrt{4+\lambda^2}}{\sqrt{y}\,\pi[\lambda^2+4y(4+\lambda^2)]}\alpha, \tag{12}$$

where the factor $\alpha=(N-1)/N$ takes into account the fact that the diagonal elements of the matrix O are excluded. This distribution fits indeed to the $N=2$ case, as demonstrated in Fig. 8. The picture is obtained for the parameter λ of the ensemble (3) equal to 0.013; the same value inserted in the above distribution gives a satisfactory agreement with the histogram. The main peak of the distribution described by Eq. (12) contains the off-diagonal elements of the orthogonal matrix O. All diagonal elements contribute to a singular peak at

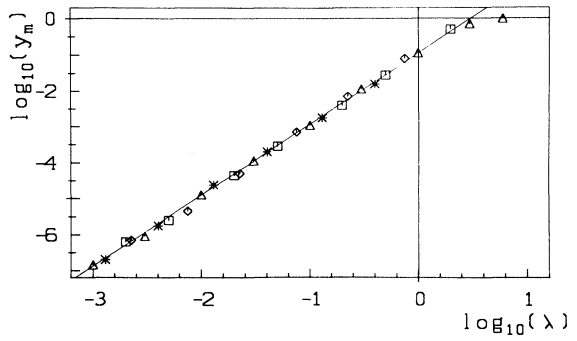

FIG. 7. Dependence of the position y_m of the peak in $P(y)$ on λ on a logarithmic scale. ($N=2$, stars; $N=20$, diamonds; $N=200$, triangles; and $N=600$, squares.)

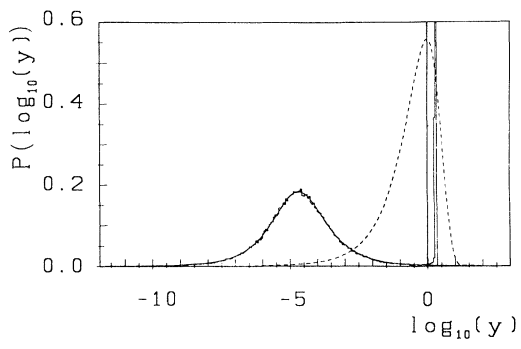

FIG. 8. Eigenvector statistics for $N=2$ and $\lambda=0.013$. The solid line stands for the distribution (12) with the same value of λ.

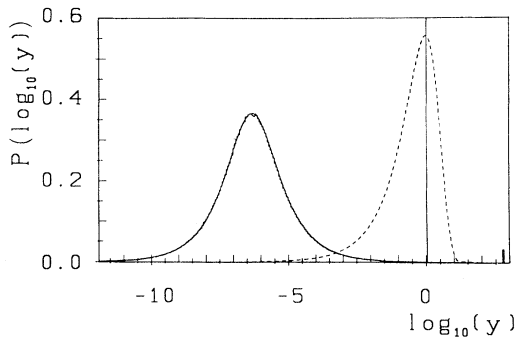

FIG. 9. As in Fig. 8 for $N=600$ and $\lambda=0.002$.

$\log_{10}(y)=\log_{10}(2)$. The distribution (12), derived for 2×2 matrices holds well for λ not larger, say, than 0.5 where the approximation (10) breaks down.

Even more interesting is the fact that this approximation works fine for an arbitrary size N of the matrices. Figure 9 presents an excellent agreement of this distribution with the histogram obtained for $N=600$ and $\lambda=0.002$. Of course, a small peak at $\log_{10}(y)=\log_{10}(600)$ corresponds to the diagonal elements of O and cannot be described by the distribution (12). Apart from that fact, the proposed distribution can be used to approximate the eigenvector statistics for all N and $\lambda<0.5$. The eigenvector statistics is, in general, basis dependent [3,28]. In the discussed model, however, the eigenvector statistics, in the basis of the unperturbed H^0, provides relevant information for an alternative study of the transition from regular to chaotic motion. In this representation, the distribution of the eigenvector components for $\lambda=0$ is a singular peak at $\log_{10}(N)$ and for $\lambda=\infty$ is given by the Porter-Thomas distribution Eq. (1b). In between these two limits our distribution, Eq. (12), describes the main peak of the distribution. Due to the large number of eigenvector components, this approach assures good statistics and may be sometimes more suitable than the standard analysis of the level-spacing distribution.

V. CONCLUSIONS

The aim of this paper was to give a thorough investigation of the often-used random-matrix model (4): the matrix H^0 is drawn from an ensemble of diagonal matrices with identically distributed matrix elements and V from the GOE ensemble. We investigated the statistical properties of the eigenvalues and the eigenvectors both of which are of interest for quantum chaos and nuclear physics. These properties, the distribution of the level spacings, and distribution of the eigenvector components, were investigated numerically with a sufficient statistics. In a first step we presented simple 2×2 predictions for the distribution of nearest-neighbor spacings and the modulus of an eigenvector component. In the next step, the high reliability of the distributions (7) and (12) was demonstrated for all N and all values of λ (with certain restrictions for the eigenvectors). We also looked for scaling laws of the model and found them for eigenvalues and eigenvectors. The eigenvalues undergo a transition from the Poisson to the Wigner distribution, with a transition rate which scales as $\sqrt{N}$. In contrast, the eigenvectors perform a universal transition independent of N from the Porter-Thomas distribution to the singular distribution of the eigenvectors of a diagonal matrix. To our knowledge, it is the first time that such an interesting difference in the behavior of the eigenvectors and eigenvalues has been shown. At first glance, a scaling proportional to $\sqrt{N}$ in the transition form a Poisson spectrum to a GOE spectrum seems to be an obstacle for a meaningful interpretation of the ensemble (5) in the context of quantum chaos. It is well know [1,23] that the bare transition parameter λ in a random-matrix ensemble (2) may possess a physical interpretation after a suitable renormalization only. On the other hand, the fitted parameter λ in the distribution (7) may have the physical meaning of an effective coupling constant since this distribution approximates well the level statistics in pseudointegrable systems [29,30].

One further impetus for our work was the paper of Cheon [20] in which he claims that there should be no scaling property in this model. We repeated his computations working with large statistics of eigenvalues and paying special attention to the dependence of the level statistics on the region in the spectrum from which the data were collected. Clear evidence of scaling was demonstrated, even using Cheon's method of momentum analysis.

At the end we mention the close similarity of our results regarding the eigenvalue distribution with the results of Caurier *et al.* [31] for a certain class of tridiagonal matrices. Their results for the nearest-neighbor distribution are identical with the lowest-order perturbative approximation for the two-level correlation function $R_2(S,\lambda)$ of ensemble (4). This approximation can be stated as follows [32]:

$$R_2(S,\lambda)=\int_0^\infty\int_0^\infty\delta\left[S-\left[\tilde{S}-\frac{4\lambda^2 y\langle\rho\rangle^2\langle H_{ij}^2\rangle}{(1+\lambda^2)}\right]^{1/2}\right]P(y)R_2(\tilde{S},0)d\tilde{S}\,dy,\quad i\neq j\ . \tag{13}$$

Here $P(y)$ is the Porter-Thomas distribution, $\langle\rho\rangle$ stands for the local mean level density, and $R_2(S,0)$ represents the correlation function of the unperturbed ensemble [for a Poisson spectrum one has $R_2(S,0)=1$]. Expression (13) gives a correct approximation of the correlation function $R_2(S,\lambda)$ in sense of perturbation theory [23] which takes account of the influence of distant levels only through the mean level density $\langle\rho\rangle$. Performing integra-

tions, we arrive at

$$R_2(S,\lambda)=\left[\frac{\pi}{8\Lambda}\right]S\exp\left[-\frac{S^2}{16\Lambda}\right]I_0\left[\frac{S^2}{16\Lambda}\right] \tag{14}$$

with

$$\Lambda=\frac{\lambda^2\langle\rho\rangle^2\langle H_{ij}^2\rangle}{(1+\lambda^2)}\ , \tag{15}$$

where $I_0(x)$ denotes the modified Bessel function. For $\lambda\ll 1$, Eq. (14) reduces to our result (7).

ACKNOWLEDGMENTS

We have enjoyed fruitful discussions with D. Forster and P. Šeba. We are grateful to H. Stöckmann and J. Stein for presenting their results before publication and supplying us with their experimental data. Financial support by the Sonderforschungsbereich Unordnung und große Fluktuationen der deutschen Forschungsgemeinschaft and by the project "Quantum Chaos" of Polski Komitet Badań Naukowych is gratefully acknowledged.

APPENDIX

We want to discuss the influence of the spectral unfolding on the resulting nearest-neighbor distribution. By spectral unfolding, we define the following transformation of the nearest-neighbor spacings:

$$S_i^{(k)}=\frac{(e_{i+1}-e_i)(2k+1)}{(e_{i+1+k}-e_{i-k})},\quad k=0,1,2,\ldots . \tag{A1}$$

It follows from this definition that the spacings are bounded from above by $2k+1$. By calculating the influence of this unfolding procedure on a Poisson spectrum, we use the fact that all eigenvalues are uncorrelated. The resulting spacing distribution reads

$$P^{(k)}(S)=\int_o^\infty\int_0^\infty\int_o^\infty\delta\left[S-\frac{\mu(2k+1)}{(\mu+k\nu+k\eta)}\right.$$
$$\left.\times P_0(\mu)P_k(\nu)P_k(\eta)d\mu\,d\nu\,d\eta\right. . \tag{A2}$$

The density distribution $P_k(S)$ is the "$k+1$"-neighbor spacing distribution, i.e., there are precisely k eigenvalues between two eigenvalues separated by distance S. These distributions are readily obtained for a Poisson spectrum

$$P_k(S)=\frac{S^{k-l}k^k}{(k-1)!}e^{-kS}\ , \tag{A3}$$

and obey the normalization $\langle S\rangle=1$. From Eqs. (A2) and (A3), we obtain the distribution

$$P^{(k)}(S)=\frac{2k}{(2k+1)}\left[1+\frac{S}{(2k+1)}\right]^{2k-1}\ , \tag{A4}$$

which allows one to find the moments

$$\langle(S^{(k)})^n\rangle=\frac{(2k+1)^n 2k\,!n\,!}{(2k+n)!} \tag{A5}$$

For the analysis of the data we had to balance two opposing tendencies: (i) to keep the finite-k effect small, (ii) to keep the stretch of the eigenvalues used by the unfolding short. We decided for $k=20$. For the moments we get, in excellent agreement with the numerical data for the Poisson limit of the ensemble (3), $\langle S^2\rangle=1.95$, $\langle S^6\rangle=507.1$, whereas for a pure Poisson spectrum we would get $\langle S^2\rangle=2.00$, $\langle S^6\rangle=720.0$. This reduction of the higher moments is relevant for the Poisson-like spectrum only since, if any repulsion of eigenvalues occurs, the k-neighbor spacing distribution ($k>1$) takes negligible values for small S.

*Permanent address: Instytut Fizyki, Uniwersytet Jagielloński, ul. Reymonta 4, 30-059 Kraków, Poland.

[1] M. L. Mehta, *Random Matrices,* 2nd ed. (Academic, New York, 1990).
[2] C. E. Porter, *Statistical Theory of Spectra: Fluctuations* (Academic Press, New York, 1965), p. 199; T. A. Brody, J. Flores, J. B. French, P. A. Mello, A. Pandey, and S. S. M. Wong, Rev. Mod. Phys. **53**, 385 (1981).
[3] M. Kuś and K. Życzkowski, Phys. Rev. A **44**, 956 (1991).
[4] F. Haake, *Quantum Signatures of Chaos* (Springer-Verlag, Berlin, 1991).
[5] M. Kuś, R. Scharf, and F. Haake, Z. Phys. B **66**, 129 (1987).
[6] R. Scharf, J. Phys. A **22**, 422 (1989).
[7] B. Dietz and F. Haake, Europhys. Lett. **9**, 9 (1989).
[8] A. Pandey, Ann. Phys. (N.Y.) **119**, 170 (1978).
[9] M. V. Berry and M. Tabor, Proc. R. Soc. London Ser. A **356**, 375 (1977).
[10] M. V. Berry and M. Robnik, J. Phys. A **17**, 2413 (1984).
[11] K. Życzkowski and G. Lenz, Z. Phys. B **82**, 299 (1991).
[12] J. B. French, V. K. B. Kota, A. Pandey, and S. Tomsovic, Ann. Phys. (N.Y.) **181**, 198 (1988); **181**, 235 (1988).
[13] M. Feingold, D. M. Leitner, and M. Wilkinson, Phys. Rev. Lett. **60**, 986 (1991).
[14] M. Wilkinson, M. Feingold, and D. M. Leitner, J. Phys. A **24**, 175 (1991).
[15] G. Casati, I. Guarneri, R. Scharf, and F. Izrailev, Phys. Rev. Lett. **64**, 5 (1990).
[16] G. Casati, L. Molinari, and F. Izrailev, Phys. Rev. Lett. **64**, 1851 (1990).
[17] S. N. Evangelou and E. N. Economou, Phys. Lett. A **151**, 345 (1990).
[18] T. Guhr and H. A. Weidenmueller, Ann. Phys. (N.Y.) **193**, 472 (1989).
[19] T. Guhr and H. A. Weidenmueller, Ann. Phys. (N.Y.) **199**, 412 (1990).
[20] T. Cheon, Phys. Rev. A **42**, 6227 (1990).
[21] G. Lenz and F. Haake, Phys. Rev. Lett. **65**, 2325 (1990).
[22] L. A. Pastur, Theor. Math. Phys. **10**, 67 (1972).
[23] A. Pandey, D. Forster, and F. Haake (unpublished); A. Pandey, Ann. Phys. (N.Y.) **134**, 110 (1981).
[24] G. Lenz and F. Haake, Phys. Rev. Lett. **67**, 1 (1991).
[25] J. Spanier and K. B. Oldham, *An Atlas of Functions* (Hemisphere, Washington, 1987).

[26] O. Bohigas and M. J. Giannoni, Ann. Phys. (N.Y.) **89**, 393 (1975).
[27] S. S. M. Wong and J. B. French, Nucl. Phys. **A198**, 188 (1972).
[28] F. Haake and K. Życzkowski, Phys. Rev. A **42**, 1013 (1990).
[29] F. Haake, G. Lenz, P. Šeba, J. Stein, H. Stöckmann, and K. Życzkowski, Phys. Rev. A **44**, 6161 (1991).
[30] P. Šeba and K. Życzkowski, Phys. Rev. A **44**, 3457 (1991).
[31] E. Caurier, B. Grammaticos, and A. Ramani, J. Phys. A **23**, 4903 (1990).
[32] S. Tomsovic, Ph.D. thesis, University of Rochester, 1986.